Earth and Space Science

RESEARCH ARTICLE
10.1029/2021EA001727

Key Points:

- Sources of precipitation for the Crimean peninsula in the Black Sea were identified using a Lagrangian approach
- The main moisture sources are Mediterranean Sea, Black Sea, and Atlantic Ocean, as well as the continental landmass via moisture recycling
- Variability in winter is partly related to the North Atlantic Oscillation. No significant temporal trends were detected over the study period

Correspondence to:
L. Langhamer,
Lukas.Langhamer@hu-berlin.de

Citation:
Langhamer, L., Dublyansky, Y., & Schneider, C. (2021). Spatial and temporal planetary boundary layer moisture-source variability of Crimean peninsula precipitation. *Earth and Space Science*, *8*, e2021EA001727. https://doi.org/10.1029/2021EA001727

Received 23 MAR 2021
Accepted 8 JUN 2021

Spatial and Temporal Planetary Boundary Layer Moisture-Source Variability of Crimean Peninsula Precipitation

Lukas Langhamer[1], Yuri Dublyansky[2], and Christoph Schneider[1]

[1]Department of Geography, Humboldt-Universität zu Berlin, Berlin, Germany, [2]University of Innsbruck, Institute of Geology, Innsbruck, Austria

Abstract The atmospheric water cycle is a key component of the global energy and moisture exchange. In order to gain better understanding of the atmospheric processes and temporal variability and trends affecting precipitation in Crimea, we use a Lagrangian moisture source detection technique based on reanalysis data from the European Center for Medium-Range Weather Forecasts. The study presents a quantitative picture of the major moisture sources that feed precipitation on the Crimean peninsula from February 1979 to January 2017. In total 51.3% of moisture stems from marine sources. Specifically, the main individual contributors are the Mediterranean Sea (15.3%), the Black Sea (14.4%), and the North Atlantic Ocean (13.9%). Continental moisture recycling contributes additional 46.9%. The amounts of moisture contribution from marine and continental sources and their respective moisture transport pathways are subject to strong seasonality. Winter precipitation in Crimea is predominantly sourced by the Mediterranean Sea. Long-term temporal trends in contribution from any of the major moisture sources are absent during the study period. Statistically significant negative correlation between the North Atlantic Oscillation (NAO) index and contribution from moisture sources exists in winter for the Mediterranean ($R = -0.22$) and Black Seas ($R = -0.23$), and for the southern continental moisture source ($R = -0.37$). The North Atlantic Ocean moisture source exhibits a statistically significant positive correlation with NAO index during spring ($R = 0.32$).

Plain Language Summary The atmospheric water cycle is a component of the global water cycle. It describes the behavior of water in the atmosphere from the evaporation in the source region to the final precipitation. This study presents a comprehensive picture of the precipitation water sources for the Crimean peninsula from 1979 to 2017. Additionally, trajectories allow to estimate travel times and pathways of air parcels. Approximately half of the Crimean precipitation originates in the marine sources: the Mediterranean Sea, Black Sea, and the North Atlantic Ocean. The other half derives from moisture recycling on the continent. Contributions from different sources vary seasonally. Despite considerable variability, there are no apparent long-term trends in contributions from any precipitation source over the 38 years period. Sources are sensitive to the North Atlantic Oscillation index, particularly during winter.

1. Introduction

1.1. Rationale

In the years following the Crimean crisis and the ensued closure in 2014 of the North Crimean Canal, which supplied water from Dnieper river into Crimea, the internal water resources of the Crimean peninsula started to fall short of meeting the economic and domestic needs of the region (Dzhamalov et al., 2018; Kayukova & Yurovsky, 2017). Discussion is ongoing regarding the ways and means of solving water shortage issues and making water management in the region more sustainable (Dzhamalov et al., 2018; Vasilenko, 2017). Meteoric precipitation, contributing to surface water and groundwater recharge is a key component of the hydrological cycle. Thorough understanding of the large-scale atmospheric conditions controlling precipitation is a prerequisite for informed and sound decisions in this respect.

The Mediterranean Sea experienced warming of the sea surface of 0.41°C per decade between 1982 and 2018 (Pisano et al., 2020). Similarly, the sea surface temperature of the Black Sea increased at 0.67°C per decade in 1982–2012 (Meredith et al., 2015; Reynolds et al., 2007). These warming trends are four to six

times higher than the global ocean warming trend of 0.11°C per decade during the period from 1971 to 2010 (Pachauri et al., 2015). A model simulation carried out by Meredith et al. (2015) showed that warming of the Black Sea surface plays an essential role in amplifying the extreme precipitation events on surrounding lands, including devastating event in 2012 in the town of Krymsk, located about 100 km east of the Crimean peninsula. Warmer sea surface temperature triggered deep moist convection, which increased precipitation by 300% in comparison to 1980s sea surface temperature (Meredith et al., 2015). Analysis of the water flux over the Mediterranean and Black Sea depicts an increasing deficit in the 1988–2005 period, due to enhanced evaporation (Romanou et al., 2010). Apparently, there are large-scale changes in the hydrological water cycle underway, and the question arises whether the observed changes of water bodies and climate affect the moisture sources and precipitation on the Crimean peninsula. In this analysis we identify moisture sources for Crimea, evaluate their coupling to large-scale processes, show characteristic synoptic patterns and indicative pathways to gain a better understanding of the atmospheric water cycle affecting Crimean's precipitation.

1.2. Physiography and Climate of Crimea

The Crimean peninsula occupies an area of 27,000 km^2. It is surrounded by the Black Sea and the Sea of Azov. The peninsula can be subdivided into two physiographic provinces, the Crimean Plains and the Crimean Mountains. The Plains occupy two thirds of the peninsula in the north. Their topography varies from fairly flat steppe to low hills. The Crimean Mountains comprise (from north to south) the Outer, the Inner, and the Main Ranges. The Outer Range gently rises from the Crimean Plains to a maximum elevation of 340 m MSL. The somewhat more prominent Inner Range reaches a maximum elevation of 560 m MSL. The Main Range comprises a series of plateaus with elevations ranging between 700 and 1,400 m MSL. In terms of its climate, Crimea can be subdivided into three regions: the Plains (semi-arid climate), the Mountains (moderately warm and humid climate), and the South Coast (Mediterranean-type climate, moderately warm with dry summers; Vyed', 1999). A somewhat finer subdivision into six mesoclimatic regions was proposed by Logvinova and Barabash (1982): I-Coastal, II-Near-shore, III-Flat steppe, IV-Hilly flats, V-Southern Piedmont, and VI-Crimean Mountains (Figure 1).

The Crimean peninsula is located in the mid-latitudes between 44° and 46°N, which results in a broad range of seasonal temperatures with maximum in July-August and minimum in January-February. For most part of Crimea located at less than ca. 200 m MSL, maximum monthly mean temperatures range between 22°C and 26°C and minimum between 0°C and 4°C (characteristic curve from the weather station Simferopol is shown in Figure 1). At highest elevations in the Crimean Mountains (weather stations Ai Petri and Angarskiy pereval), seasonal temperature profiles have similar shape, but both maximum and minimum values are lower (14°C to 16°C and −4°C to −1°C, respectively). The Crimean Mountains range has an important function as an orographic barrier for approaching air masses. It serves as a moisture divide, which influences the precipitation pattern over Crimea. The monthly precipitation amounts exhibit considerable spatial variability and range between 370 mm yr^{-1} in the northern steppe parts of the peninsula and 918 mm yr^{-1} in the Crimean Mountains (Figure 1). The orographically induced precipitation increase is estimated by Vyed' (2000) as 60 mm per 100 m of altitude.

At the weather station Simferopol, over the period covered by this study (February 1979 to January 2017), the monthly average temperatures show a statistically significant ($p < 0.05$) growth of 0.67°C per decade (Figure 2). It should be noted, that the positive temperature trend became characteristic of this part of Crimea since the 1980s. Before that, from 1900s, there was no long-term temperature trend (Ergina & Zhuk, 2019). In contrast, the monthly precipitation amounts show no statistically significant systematic change between 1979 and 2017. This stable precipitation pattern has established around 1950s; up to 100 mm lower mean annual precipitation amounts were observed before that, between mid-1880s and 1940s (Ergina & Zhuk, 2019).

The state of the knowledge regarding the origins of air masses arriving to the Crimean peninsula is presented in Vyed' (2000). According to this author, about 75% of the air masses arriving to Crimea originate from the Atlantic Ocean. The mid-latitude cyclones are driven by westerly winds either across continental Europe or across the Mediterranean Sea. Some 10% of the Crimean air masses relate to periodic invasions of cold fronts from northern latitudes. Additional 8% represent warm and moist air from the Mediterranean

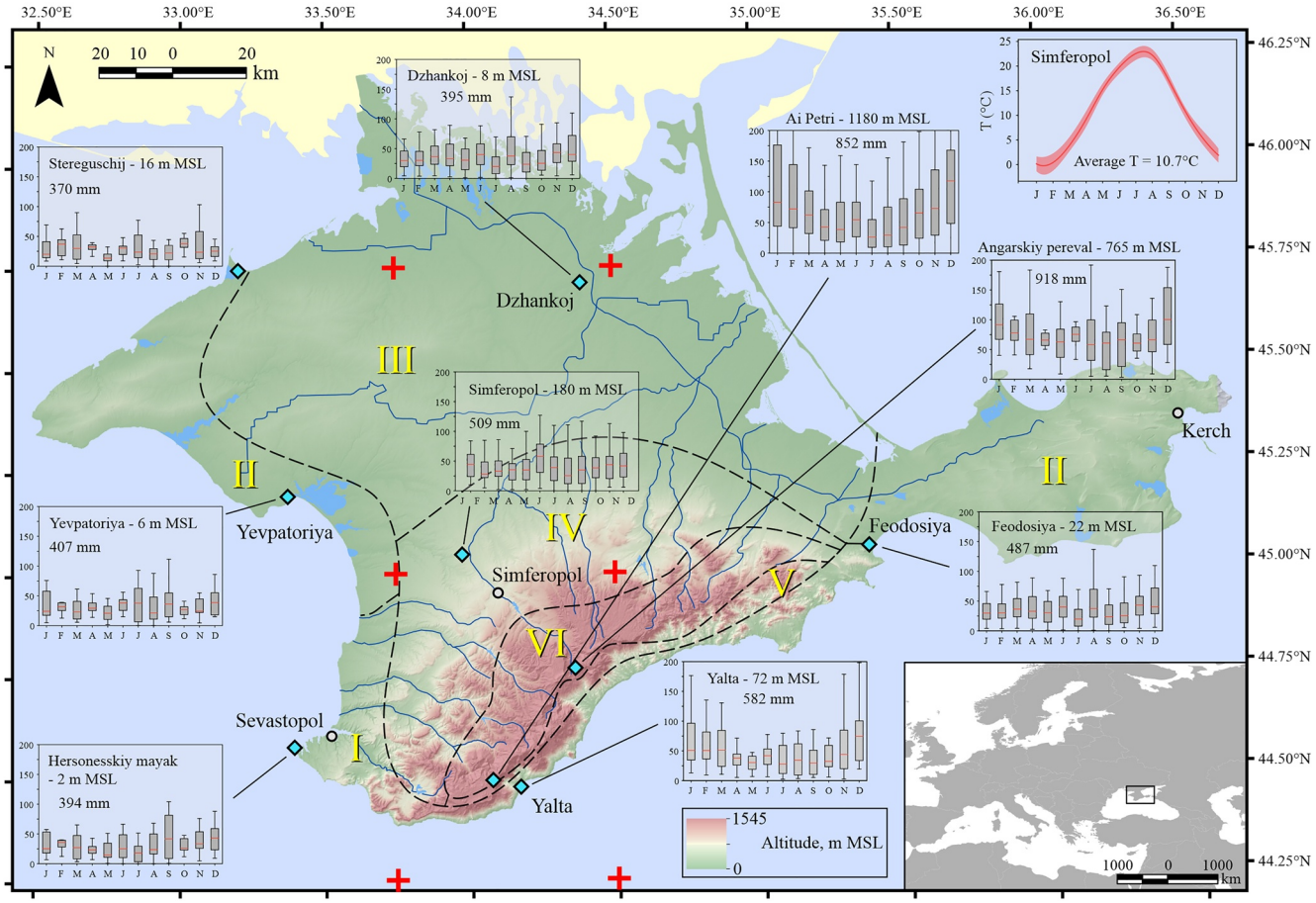

Figure 1. Physiography and climate of the Crimean peninsula. The dashed lines constrain the six mesoclimatic regions after Logvinova and Barabash (1982): I-Coastal; II-Near-shore; III-Flat steppe; IV-Hilly flats; V-Southern Piedmont; and VI-Crimean Mountains. The diagrams of the monthly precipitation amounts (mm) are compiled from WMO-compliant weather stations (cyan diamonds) in the period from 1979 to 2017. The mean annual precipitation amounts are indicated. The annual temperature curve is shown for Simferopol station. Six red crosses show the starting locations of the backward trajectories, which constrain the target area of this study.

Sea, and the remaining 7% are dry air originating from Asia. Overall, the air circulation patterns appear to be highly variable and air masses bringing moisture to Crimea may follow different pathways.

Vyed' (2000) estimated the contributions using an Eulerian perspective, by considering only the air advection to the Crimean peninsula. More precise technique is required to estimate the trajectories of air masses and sources of moisture associated with them. Instead of considering the state of the atmosphere at a particular locality at any given time, one can follow the temporal changes of an air parcel along its trajectory. This approach constitutes a change from Eulerian to Lagrangian perspective. If the moisture change is traced along the trajectory, the moisture sources and sinks can be detected (Stohl & James, 2004). In this study we determine the main moisture sources of the Crimean peninsula and their variability from 1979 to 2017 by using a Lagrangian perspective based on a numerical weather prediction model.

2. Materials and Methods

Numerical weather prediction models describe physical processes in the atmosphere by a set of partial differential equations (Kalnay, 2003). These equations are spatially discretized on a regular grid so that the state of the atmosphere at any given time is known. By monitoring the change of state variables at a given grid point, after a while the observer notices changes due to advection of air. This reflects environmental changes in the Eulerian perspective. If we are interested in the change of state variables within a particular

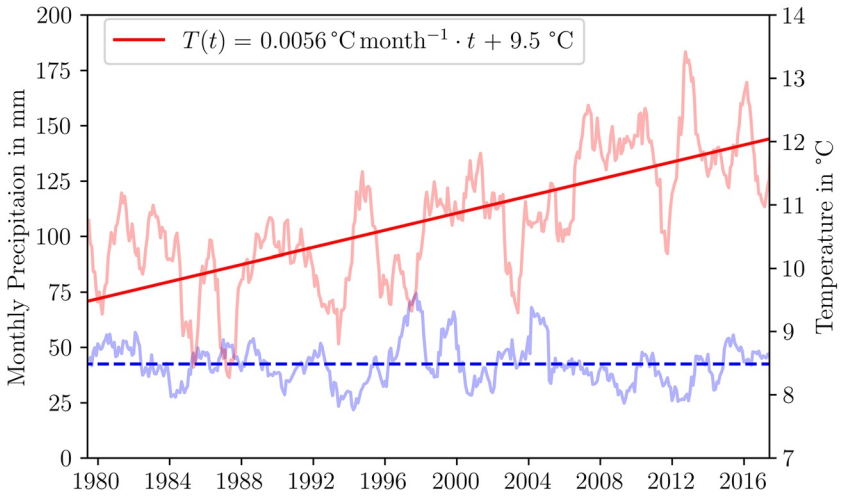

Figure 2. 1-year centered rolling mean of the monthly mean temperature (light red) and the monthly precipitation sum (light blue) from the meteorological station Simferopol. A significant (95% confidence interval) linear temporal trend only exists for temperature (solid red line). The dashed blue line indicates the monthly mean precipitation averaged over the time period from 1979 to 2017.

air parcel over time, we can convert the Eulerian three-dimensional (3-D) wind field $\vec{u} = (u, v, w)$ into a Lagrangian perspective $\vec{x} = (\lambda, \phi, p)$ in spherical coordinates,

$$\frac{\mathrm{D}\vec{x}}{\mathrm{D}t} = \vec{u}(x). \tag{1}$$

By integrating the wind field $\vec{u}$ we get a trajectory $\vec{x}(t)$. This conversion is realized by the Lagrangian analysis tool LAGRANTO (Wernli & Davies, 1997), which integrates Equation 1 numerically in three iteration steps. A detailed description of LAGRANTO can be found in (Sprenger & Wernli, 2015). For a survey and a comparison of the most common trajectory models we refer to Stohl et al. (2001).

2.1. Moisture Source Diagnostic Technique

In this study, we use the moisture source diagnostic technique developed by Sodemann et al. (2008), which relies on the basic concept developed by Stohl and James (2004): In an air parcel in which the formation of ice crystals and water droplets is neglected, the specific humidity q is conserved along a trajectory $\vec{x}(t)$. An air parcel of any given mass m exhibits an increase of the specific humidity only by moisture uptake within the planetary boundary layer (PBL) through terrestrial evapotranspiration, and a decrease by precipitation during a time interval dt (Stohl & James, 2004),

$$m\frac{\mathrm{d}q}{\mathrm{d}t} = E - P. \tag{2}$$

This concept does not consider individual moisture uptake and precipitation events which can occur along a trajectory during any time interval $\mathrm{d}t = 6$ h. The average of the moisture changes within the time interval is considered instead. Whenever the specific humidity of the trajectory increases ($\mathrm{d}q > 0$) within the scaled PBL, a moisture source is identified (Sodemann et al., 2008). The amount of moisture uptake is attributed to the Earth's surface and interpolated on a 1.0° grid. During a backward trajectory calculation, the trajectory may have multiple moisture uptakes. Therefore, all moisture uptakes are weighted relative to the pre-existing moisture. Precipitation en-route reduces the influence of previously estimated moisture sources and is subtracted according to their contribution (Sodemann et al., 2008). Comparison based on a case study for Europe (Winschall et al., 2014) shows that the Lagrangian moisture-source detection method yields results that are similar to the outcomes of more complex Eulerian approaches. This provides a validation of the Sodemann et al. (2008) method and its suitability for a comprehensive climatological analysis.

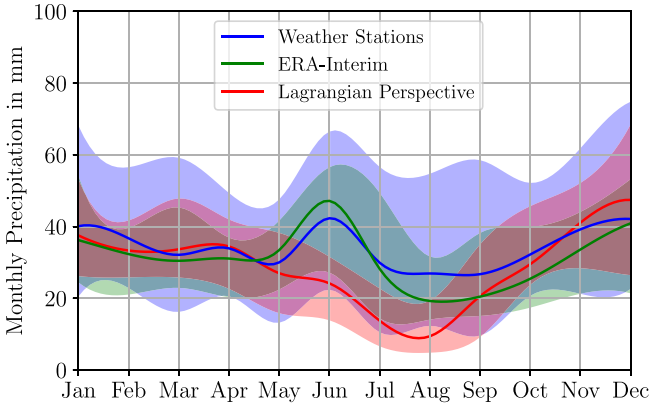

Figure 3. Comparison of the monthly precipitation amounts measured at the Crimean weather stations (cf. Figure 1), obtained from ERA-Interim, and derived from the Lagrangian model. The solid lines show the median; the filled area corresponds to the inner-quantile range.

2.2. Model Setup

The global reanalysis product ERA-Interim provided by the European Center for Medium-Range Weather Forecasts (Berrisford et al., 2011; Dee et al., 2011; Owens & Hewson, 2018) constitutes the base for the trajectory calculation. The required fields are the 3-D wind vector, the temperature, the specific humidity, the logarithmic surface pressure, the 2-m air temperature and height of the PBL. This study covers the fields from 10° to 90°N in a horizontal resolution of 1.0° at all 60 available model levels in the time interval of 6 h from 1979 to 2017. The start positions of the trajectories are located at the nodes of a regular horizontal grid of 0.75° resolution, which is present in 11 equidistant pressure levels (49.9 hPa) from the surface to 500 hPa above the ground level. In the plane, the six starting grid points were placed between 33.75°–34.5°E and 44.25°–45.75°N. The resulting rectangular target area "samples," to various extent, most of the Crimean mesoclimatic regions (Figure 1).

Calculation of 66 (6 × 11 starting positions) backward trajectories was initialized in a 6 h time interval. The backward calculation time was set to 15 days, which keeps the amount of preexisting moisture small (<5%). Once a trajectory intersects the model surface, the trajectory is shifted upwards by 10 hPa. This rather pragmatic option accommodates the nature of the turbulent mixed PBL. The conversion of the PBL height into pressure coordinates is realized by the US-standard atmosphere with a constant lapse rate of 6.5 K km^{-1} and the respective 2-m temperature as described in Langhamer et al. (2018).

The Lagrangian precipitation estimate P calculated by Equation 2 was converted from the specific humidity decrease of each respective starting location $\Delta q(t_0)$ in g/kg into the 6 h accumulated sum in mm according to,

$$P = \frac{1}{g}\sum_k \Delta q_k(t_0) \cdot 10^{-3} \cdot \Delta p_k, \tag{3}$$

with the gravitational acceleration g, and the vertical extent of an air parcel Δp_k which is in this case 4,990 Pa. Monthly precipitation amounts estimated by the trajectories (Equation 3) are presented in Figure 3 and compared to the outputs of the ERA-Interim total precipitation and measurements from weather stations. Observations of monthly precipitation amounts are derived from the database of the National Oceanic and Atmospheric Administration National Centers for Environmental Information (https://www.ncdc.noaa.gov/cdo-web/datatools/findstation). The location of the weather stations is provided in Figure 1. Additional information on weather stations is given in Table 1.

2.3. Model Performance

Figure 3 compares the monthly precipitation amounts of ERA-Interim, from available weather stations in Crimea (Table 1), and of the Lagrangian perspective (Equation 3). Both, the weather stations and ERA-Interim data, exhibit a statistically significant ($p < 0.05$) conformance of the monthly precipitation amount ($R^2 = 0.79$). In complex mountainous terrain, ERA-Interim does not capture micro-scale features in all detail (Gao et al., 2012). ERA-Interim underestimates monthly precipitation mean at Crimea by 9%.

Table 1
WMO Compliant Weather Stations in Crimea, Used in This Study

Station	Simferopol	Ai Petri	Yalta	Hersonesskiy mayak	Yevpatoriya	Stereguschij	Dzhankoj	Angarskiy pereval	Feodosiya
WMO-number	339460	339990	339900	338840	339290	339210	339340	339580	339760
Data coverage	100%	100%	59%	78%	77%	100%	66%	83%	77%

Note. The data coverage describes the available monthly precipitation data over the period from 1979 to 2017.

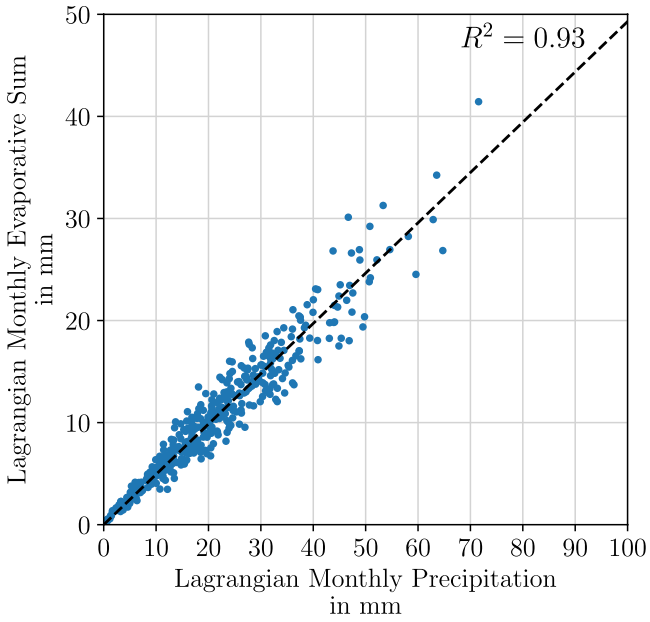

Figure 4. The Lagrangian monthly precipitation (Equation 3) and the monthly amount of all identifiable moisture sources.

The precipitation amounts calculated by Equation 3 estimate the precipitation derived by the Lagrangian model contributing to the target area. For the cold period of the year, the Lagrangian estimated monthly precipitation exhibit good agreement with the ERA-Interim based precipitation. For summer months, the Lagrangian approach underestimates precipitation by up to 50%. This may be explained by the increasing role of convective precipitation mechanism during warmer months of the year. Sub-grid scale processes are not captured by the moisture source identification technique (Equation 2). In numerical weather prediction models processes at the sub-grid scale, such as convective precipitation, are parameterized. The 3D wind field required for the Lagrangian perspective (Equation 1), and thus the large-scale flow remain applicable. Accordingly, only the absolute amounts of evaporation for the summer season should be treated with caution. Thus, amounts of the respective moisture source will be presented as relative contributions.

Figure 4 evaluates the efficiency of the Lagrangian moisture source detection technique. A statistically significant linear correlation between the monthly evaporative sum and the Lagrangian precipitation estimate is apparent ($R^2 = 0.93$). Notice, that moisture uptakes from above the PBL (41%) and pre-existing moisture at the trajectory end position (5%) can't be assigned to Earth's surface. They are not considered in this study, which results in the lower monthly evaporative sum compared to the estimated precipitation. The monthly detection efficiency ranges between 29% and 79% with a seasonal cycle less than 6.6% and the highest efficiency in March and April.

3. Moisture Sources

3.1. The 38-Years Climatological Mean

Figure 5 presents a diagnostic picture of the mean moisture sources for the Crimean peninsula for the period February 1979 to January 2017. Only moisture uptakes within the scaled PBL are considered which contributed to the precipitation at the peninsula. Moisture uptake locations close to the trajectory starting positions (target area) have the highest evaporative contributions, ranging up to 0.044 mm month^{-1} per grid point. The areas of highest uptakes include the Black Sea and the Sea of Azov. In addition, the Mediterranean and North-western parts of Caspian Sea show an evaporative contribution of up to 0.02 mm month^{-1}. Apparently, substantial amounts of moisture originate from the continent. Because this moisture cannot be directly linked to a specific hydrological moisture source, we designate this as continental moisture recycling. According to the 38-years average of the 800 hPa geopotential height, air masses are predominantly advected by westerlies. Note that some moisture sources, such as Atlantic Ocean for example, are not visible in Figure 5 because the contributions of individual grid points cannot be rendered at the chosen color scale. This graph illustrates the moisture uptake per grid point. In other words, it shows the intensity of moisture uptake. In order to assess quantitative contributions of different sources to precipitation at the target area, we need to additionally consider the areas of these sources. For this purpose, we define 8 major moisture uptake regions (Figure 6). The marine moisture sources comprise the northern part of the Atlantic Ocean, as well as inner seas: Mediterranean, Black, Caspian, Baltic, and Sea of Azov. Since the collective moisture contribution of the Irish Sea, the North Sea, and the Norwegian Sea is less than 1%, for the sake of simplicity those regions were assigned to the Atlantic Ocean. The continental moisture sources are subdivided into Europe and a southern part, which encompasses northern parts of Africa and Asia, and Arabian Peninsula, designated as AAA source region.

The respective moisture source contribution, as well as travel times of the air parcels are presented in Figure 7. In order to eliminate any weighting of the monthly estimated moisture source from any given region as a result of the amount of monthly precipitation sum in the study area, we calculate their relative contribution that describes the monthly portion of moisture from each defined moisture source region (Figure 6)

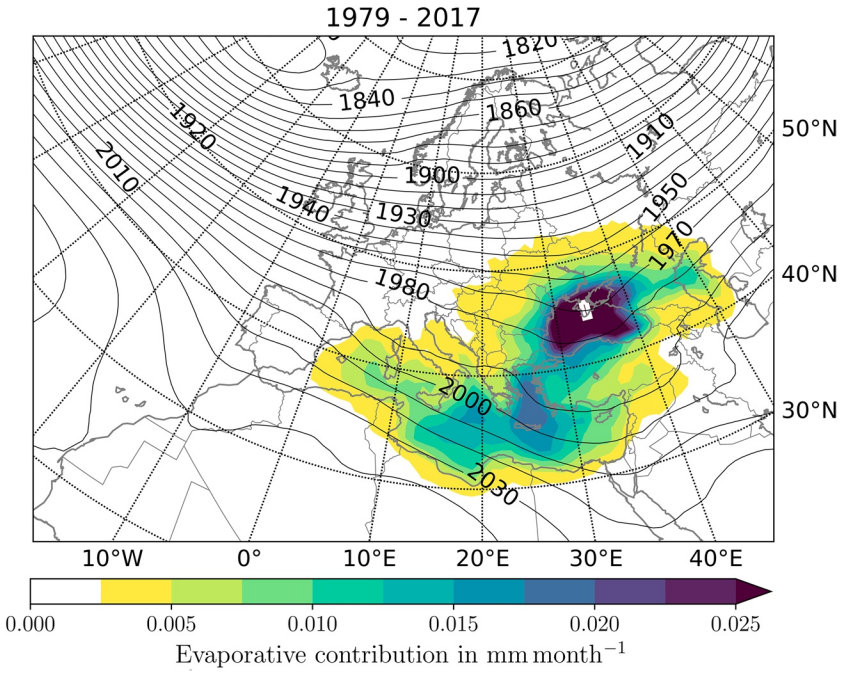

Figure 5. Monthly mean moisture uptakes per grid point (1.0° resolution) which contribute to the precipitation at the target area on the Crimean peninsula (white rectangle) over a 38-years period. Uptake that exceed the color bar have a maximum value of 0.044 mm month^{-1}. Solid lines indicate the average 800 hPa geopotential height in meters.

in relation to the total identified moisture, respectively. According to a Shapiro-Wilk normality test (Shapiro & Wilk, 1965) the results are not normally distributed. Thus, in order to calculate the mean of the non-parametric distribution we apply a bootstrapping method to estimate the 95% confidence interval (significance level of 0.05) of the results (Wilks, 2011). In addition to the actual value, the confidence interval is written in brackets behind to indicate its uncertainty.

We subdivide the moisture contributors into marine and continental moisture sources. Among the marine moisture sources the three main contributors are: The Mediterranean Sea with 15.3(13.9, 16.6)%, the Black Sea with 14.4(13.6, 15.2)% and the Atlantic Ocean with 13.9(12.7, 15.1)%. The Atlantic Ocean source comprises a very large area making it the third largest contributor out of marine moisture sources, despite small moisture uptakes (all <0.0025 mm month^{-1} per grid point).

Continental moisture sources operate through evapotranspiration or "recycling" of moisture originally derived from marine sources. Moisture recycling plays a major role in feeding precipitation over Crimea: 46.9[45.1, 48.6]% of the detectable moisture originates from continents of which 32.0[30.4, 33.7]% originates from Europe and 14.9[13.9, 15.8]% from Anatolia and northern parts of Africa and Asia. Areas in the direct vicinity of Crimea show the highest evaporative contribution (Figure 5). This can be explained by virtually

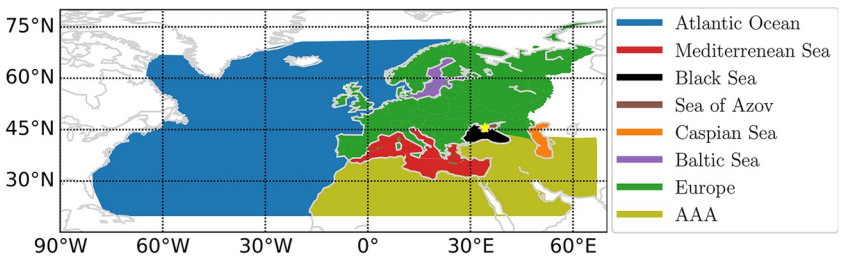

Figure 6. The moisture source regions defined for analysis. The yellow star shows the target area.

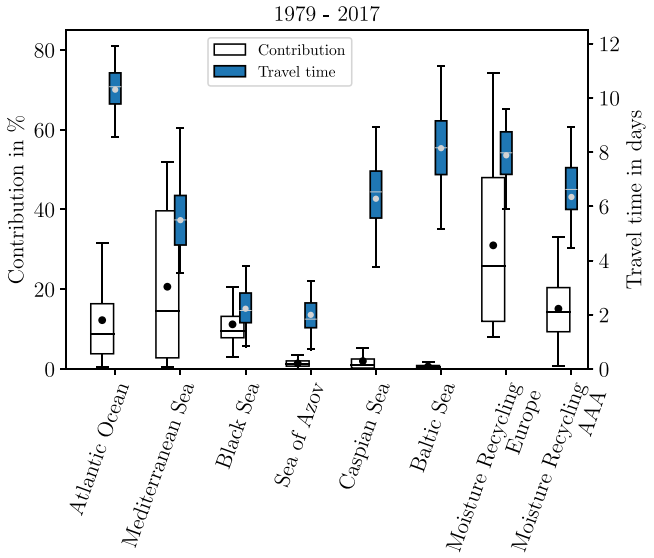

Figure 7. Contribution of moisture source regions (cf. Figure 6) and average travel times of air parcels from their moisture source regions to the target area in the Crimean peninsula. The boxplots indicate the 95% confidence interval (whiskers), the interquartile range (boxes), the median (horizontal line) and the mean (circle).

absent en-route precipitation and the highest density of trajectories in this area. Advection of air to the Crimean peninsula is driven primarily by the westerlies. Thus, moisture from the Baltic Sea, as well as Caspian Sea and Sea of Azov account for a very small share of the Crimean precipitation. In total, these marine sources contribute 4.3[4.0, 4.6]% of the detectable moisture.

The travel times of the air parcels provide more in-depth information about the air advection. For example, moisture originating from the Black Sea arrives to Crimea within 0.9–3.6 days (95% confidence interval). A low gradient of the 800 hPa geopotential height occurs between the Crimean peninsula and the Mediterranean Sea. There are particular synoptic situations where moisture is advected directly from the Mediterranean Sea by the subtropical jet. Thus, the 95% confidence interval of travel times covers a wide range of 0.8–9.2 days at the Mediterranean Sea. The travel times of the moist air parcels originating from the Atlantic Ocean (7.9–11.7 days) approach the residence time of water in the atmosphere (8–10 days van der Ent & Tuinenburg, 2017).

3.2. Inter- and Intra-Annual Variability of Moisture Sources

To investigate the seasonal changes of moisture source contributions, the averages for the corresponding months are calculated for the period from February 1979 to January 2017. In this study, winter refers to the months December, January, February (DJF), spring to March, April, May (MAM), summer to July, June, August (JJA), and autumn to September, October, November (SON).

Figure 8 shows diagnostic pictures and the respective contributions of the moisture sources for each season. Winter is characterized by a southward excursion of the westerly storm track (Figure 8a). Cyclones arriving from south and southwest transport marine subtropical air from the Mediterranean Sea. The majority of moisture originates from the Mediterranean Sea (29.6[27.3, 32.0]%; Figure 8b). This is likely related to a thermal effect between the relatively warm air masses above the sea surface surrounded by cold continental air masses. When relatively cold continental air masses are advected over the relatively warm Mediterranean Sea surface this can trigger convection. The instability is indicated by the cyclonic curvature of the 800 hPa geopotential height over the Mediterranean Sea which is characteristic during winter. This synoptic pattern favors lee cyclogenesis and enhances the baroclinic instability south of the Alps (Buzzi & Tibaldi, 1978). Thus, the Mediterranean Sea has the highest density of cyclones and the deepest central thickness of their depression during winter months (Campins et al., 2011). According to Campins et al. (2011) cyclogenesis over the Mediterranean Sea dominates in the Aegean Sea during cold seasons and one of their favored tracks is northeastward to the Black Sea. This is consistent with the 800 hPa geopotential height pattern which indicates enhanced cyclonic curvature between Aegean Sea and Black Sea during winter months. On average, more moisture is advected by south-westerlies towards the Crimean peninsula. The average travel time of upstream sources within the core zone of the westerlies becomes shorter during winter months. Moisture supply from the Atlantic Ocean is enhanced and shows its highest contribution during winter months (27.3[24.8, 29.6]%). The increased moist air advection from the Atlantic Ocean might be explained by two mechanisms. First, the low-level jet axis reach further south and moist air advection by the westerlies may be enhanced during winter months, which increases the zonal moisture fluxes. Second, the convection over land surface may be inhibited during the cold months, which may result in diminishing continental moisture contribution and less en-route precipitation.

Spring shows a transition phase regarding the large-scale flow and moisture sources from the winter to the summer seasons (Figures 8c and 8d). The large-scale circulation is characterized by diminishing strength of the westerlies. The latter give way to southern and southwestern cyclones, which transport warm air from the Mediterranean Sea, the Black Sea and the southern continental land masses towards Crimea. The annual maximum of southern continental moisture sources is remarkable: according to (Campins et al., 2011)

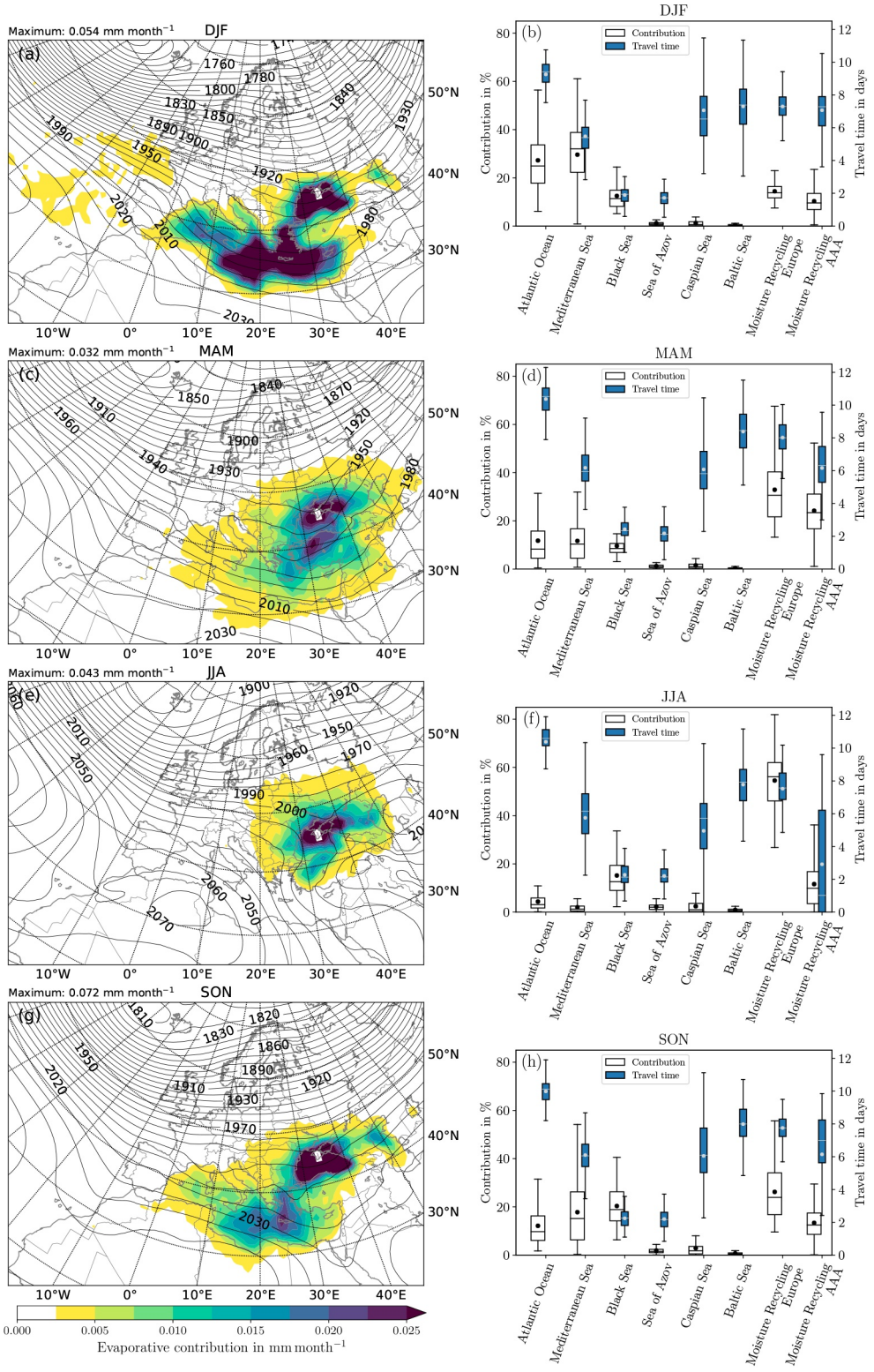

Figure 8. Left: Moisture sources during different seasons. The maximum moisture uptake per grid point is indicated in the header of each plot. Right: Contributions of the moisture source regions (cf. Figure 6) and mean travel times of air parcels. The boxplots indicate the 95% confidence interval (whiskers), the interquartile range (boxes), the median (horizontal line) and the mean (circle).

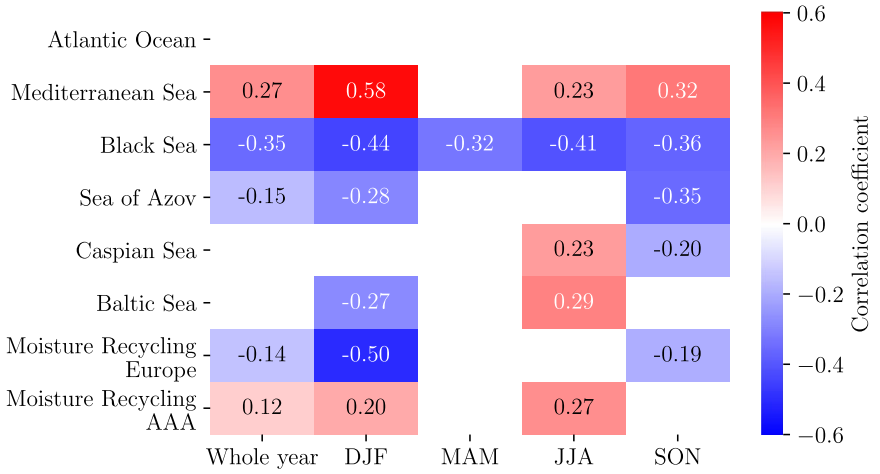

Figure 9. Correlation between moisture uptakes from the defined source regions (cf. Figure 6) and precipitation on the Crimean peninsula based on ERA-Interim. Spearman rank-order correlation coefficients are calculated for the whole year and individual seasons. Only statistically significant ($p \leq 0.05$) coefficients are shown.

the cyclone density is the highest during spring over the Anatolian Plateau. The relatively low geopotential gradient and the west-southwesterly mean air flow favor air advection from the south. Consequently, continental moisture recycling from the Anatolian Plateau is prominent during spring.

Summer circulation is commonly affected by a predominant high-pressure ridge extending from the Mediterranean to the Caspian Sea (Figure 8e). Due to the interaction of the surface temperatures of the Sea of Azov, Black Sea, and the land masses, the pressure gradient diminishes in summer, initiating local southwestern winds, northern night sea breezes and sporadic northeast storms. The absence of a pressure gradient is apparent in the 800 hPa geopotential height over the Crimean peninsula. The latter is located between a ridge axis over south-east Europe, and an anti-cyclone with its center in the vicinity of the Caspian Sea. These conditions favor air advection from continental areas, where moisture recycling is at a maximum and long-range transport of moisture is almost absent (Figure 8f). Thermal heating over continents and southward excursions of upper level troughs triggers convection and meso-cyclones above lands surface which are mostly developing during summer. Amounts of moisture supplied from the European continent in summer reach 54.6[52.3, 56.8]%, providing the strongest contribution to precipitation at the Crimean peninsula. Enhanced evapotranspiration and distinctive convection cells in the PBL amplify vertical moisture flux at the Earth's surface. The sub-tropical anti-cyclones reach north of 30°N. This favors large-scale subsidence and north-westerly flow over the Mediterranean. The resulting characteristic pattern prevents air advection from the Atlantic Ocean and the Mediterranean Sea. Hence, these major marine moisture sources contribute little to the Crimean precipitation in the summer months.

Circulation in autumn is similar to that in spring but features different major moisture sources (Figures 8g and 8h). The difference between these transition seasons is a result of warmer sea surface and higher air temperatures during autumn. Thus, the Black Sea (20.4[18.7, 22.0]%) and the Mediterranean Sea (17.8[15.3, 20.3]%) are the most important marine moisture sources in autumn. The continental moisture recycling contributes 39.6[37.6, 41.6]%.

Possible correlations between the contribution of each defined moisture source region and Crimean precipitation amounts are investigated with a Spearman rank-order test (Figure 9). There is no significant correlations between the Atlantic Ocean moisture source and Crimean's precipitation. Thus, the moisture contribution of the Atlantic Ocean and the associated large-scale zonal moisture transport is rather stable. This holds true even in winter, although we have concluded the Atlantic Ocean to be the main contributor during this time of year. Prevailing westerlies and en-route precipitation attenuate the relevance of the North Atlantic moisture source in controlling Crimea's monthly precipitation amounts. In contrast, the Mediterranean Sea shows a statistically significant positive correlation with the monthly precipitation amount of Crimea in all seasons excluding spring. During winter, contribution of the Mediterranean Sea

increases for months with larger precipitation amounts. In accordance with results of Ciric et al. (2018), moisture sources from the Mediterranean Sea play a dominant role for moist winter months. A somewhat weaker positive correlation also exists for the continental moisture recycling from the south (AAA). Extra-tropical cyclones passing North Africa and the Mediterranean Sea might be one of the driving forces, and might be associated with warm conveyor belts which are responsible for >60% of the monthly precipitation extremes in the region of the Crimean peninsula (Pfahl et al., 2014). The finding provides a hint at the favored track of atmospheric rivers during winter, an aspect which has not been studied yet. The Black Sea source shows negative correlation with the precipitation at the target area during all seasons. Respectively, during drier months, substantially more moisture stems from local sources such as the Black Sea. Drier winter favor moisture advection from the European Continent. Sea of Azov, Caspian Sea and Baltic Sea are minor moisture contributors (in total <3%) but underline the crucial role of favored moist air advection. For instance, during summer months the 800 hPa geopotential height indicates the lowest gradient over the Crimean peninsula in comparison to other seasons (Figure 8e). The Crimean peninsula is located between one cyclone centered at Algeria, and an anti-cyclone with its center in the vicinity of the Caspian Sea. This causes a splitting of the westerlies with the Crimean peninsula being located in between. The two branches are the mid-latitude westerlies and the south-westerly subtropical low-level jet. A predominant air advection is absent at the Crimean peninsula, and the interplay of the cyclone and anti-cyclone controls moist air advection to Crimea. Hence, the amount of precipitation is positively correlated with air advection from all directions during summer other than the Black Sea area.

3.3. Moisture Source Time-Series From 1979 to 2017 and Teleconnection to the North Atlantic Oscillation

The time series of moisture supply from all source regions are presented in Figure 10. To illustrate the absolute changes of moisture supply from each moisture source area, absolute amounts of the monthly moisture contribution were plotted. In contrast to the reported sea surface warming trend of the Mediterranean and Black Seas (e.g., Meredith et al., 2015; Pisano et al., 2020), temporal changes of evaporation and precipitation (Romanou et al., 2010; Skliris et al., 2018; Voskresenskaya & Vyshkvarkova, 2016), and observations of a multi-decadal salinification of the Mediterranean Sea (Skliris et al., 2018), no statistical significant trend can be identified for any major moisture source region from 1979 to 2017 by a non-parametric Mann-Kendall test. Meredith et al. (2015) hypothesized amplification of convective precipitation events in Mediterranean and Black Sea coastal regions due to the sea surface warming. A linear trend analysis of the number of days with extreme precipitation in Crimea indicate a spatially heterogeneous pattern (Voskresenskaya & Vyshkvarkova, 2016). An increasing trend is only visible during summer in Southern Piedmont. Analysis of the freshwater budget over the Mediterranean and Black Seas indicates an increasing deficit owing to increased evaporation (Romanou et al., 2010). However, an increasing evaporation trend over the sea surface does not necessarily imply an increasing trend of precipitation over the surrounding land masses. There is no evidence of a statistically significant trend in monthly precipitation amounts within the target area during the past decades neither from weather station data nor from ERA-Interim precipitation in the study area. In addition, the occurrence of extreme precipitation months considering the 90% percentile is not increasing (not shown), as could be inferred (incorrectly) from the studies of Meredith et al. (2015). In fact, the occurrence of extreme winter and summer precipitation events shows a predominantly decreasing linear trend over the Crimean peninsula from 1951 to 2009 (Voskresenskaya & Vyshkvarkova, 2016).

Further, we investigated the interplay between moisture source variability and large-scale flow patterns. The North Atlantic Oscillation (NAO) is a prominent and recurrent atmospheric oscillation pattern of the North Atlantic effecting the climate in large parts of Europe (e.g., Hurrell et al., 2003; Trigo et al., 2002; Vicente-Serrano & López-Moreno, 2008; Wanner et al., 2001). Its variability is expressed by an index which quantifies the strength and location of the westerly storm track. Hence, different phases lead to anomalies of the meridional and zonal heat and moisture transport and influence temperature and precipitation patterns in eastern North-America and western and central Europe, particularly during winter months (Hurrell, 1995). The NAO phase is quantified by an index. A positive (negative) NAO phase is associated with a weakening (strengthening) of the westerly storm track over the Atlantic Ocean. Considering the Crimean peninsula, statistically significant ($p < 0.05$) weak negative correlations between the NAO index and the ERA-interim precipitation exists only during winter (DJF) in the period from 1979 to 2017 ($R = -0.22$).

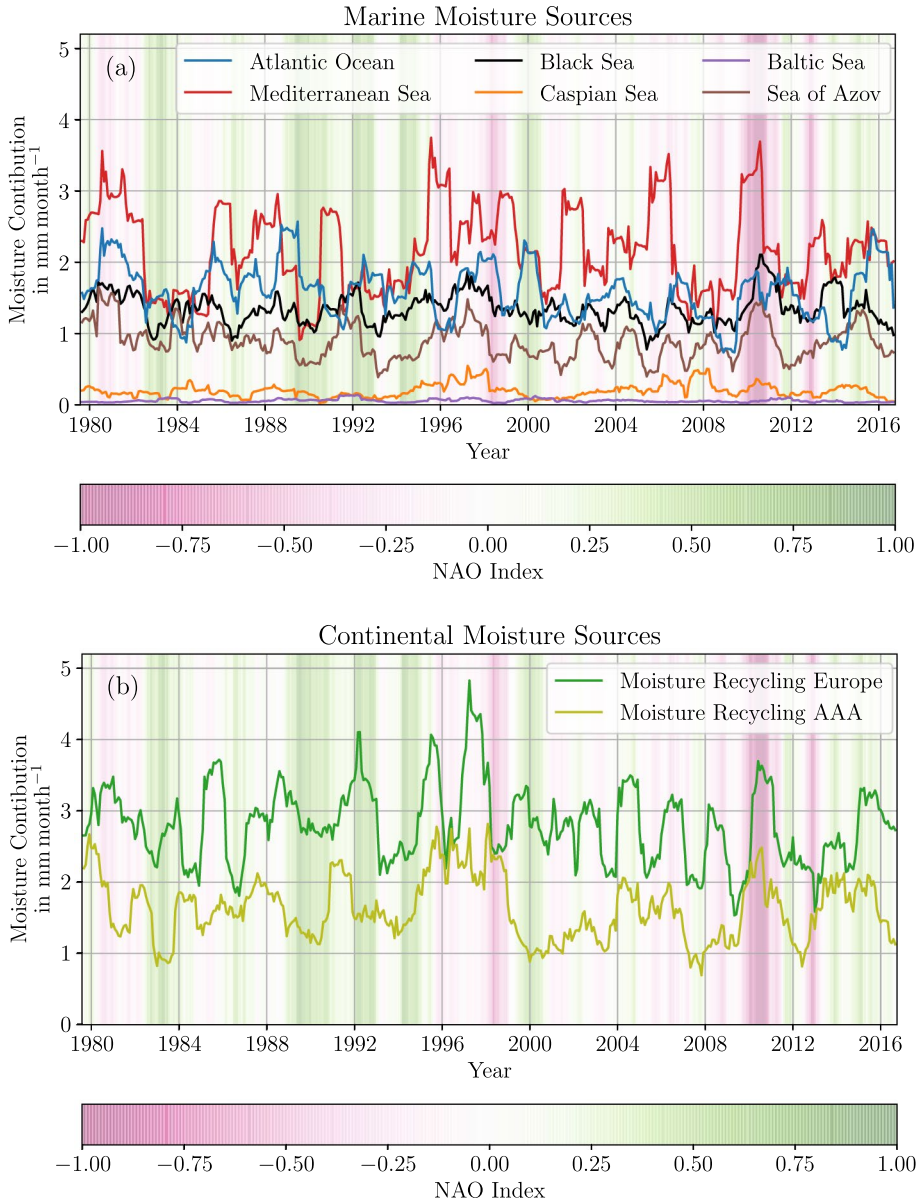

Figure 10. Temporal evolution of the absolute moisture contribution from marine (a) and continental (b) moisture sources and the North Atlantic Oscillation (NAO) index. The monthly data is smoothed (12-months rolling mean).

Likewise, only during the winter months the moisture contributions from the Mediterranean ($R = -0.22$), the Black Sea ($R = -0.23$), and the AAA source region ($R = -0.37$) exhibit a significant negative correlation with the NAO index. In summary during the course of a year, the NAO phase affects precipitation and moisture sources contribution of Crimea only during winter. This is in agreement with stable isotope measurements in precipitation from the Crimean Piedmont and the Crimean Mountains which show a significant negative correlation with NAO only during cold periods of the year (November, December, January, February, and March; Dublyansky et al., 2018). There is no indication for a response of moisture sources from the Atlantic Ocean to NAO during winter. A significant dependence between the NAO index and moisture supply from the Atlantic Ocean appears only in spring ($R = 0.32$).

4. Technical Limitations of the Moisture Source Detection Method

The trajectory calculations are based on the reanalysis product ERA-Interim. Neither the complex mountain terrain nor small micro-scale features can be depicted by the numerical weather prediction model. However, for a monthly resolved moisture source analysis discussing phenomena at scales from 10^2 km to 10^4 km, local differences due to sub-grid scale features can be neglected. ERA-Interim is able to depict the characteristic annual monthly precipitation pattern (Figure 3). The Lagrangian approach underestimates precipitation in summer. Therefore, absolute evaporative moisture amounts for June, July, and August should be treated with caution (Figures 8e and 10). However, the results shown in Figure 8f are not affected by this. The Lagrangian approach underestimates precipitation proportionally at all moisture sources. Therefore, the relative contributions of the moisture sources, determined from the absolute identifiable amounts of moisture, remain valid.

Trajectory calculations are run at 6 h-intervals, which is defined by the temporal resolution of ERA-Interim data. Any moisture sources between one trajectory calculation time step are all assigned to the new estimated trajectory position. This simplification shifts each moisture uptake area in direction of the flow. This might effect rendering of moisture sources located near the coastline, which become assigned to continental moisture sources. The effect cannot be quantified for the whole analysis and is assumed to be negligibly small. Additionally, moisture increase and moisture loss may occur during a 6 h calculation interval. The Lagrangian methodology allows only to consider the absolute difference of the specific humidity between a calculation interval and assigns it to either evaporation or precipitation (Equation 2).

Pre-existing moisture (beyond the 15 days backward trajectory calculation) accounts for 5% of the total Lagrangian estimated precipitation. The results presented in Figure 8 indicate that identified moisture uptake locations before 13 days contribute very little. Therefore, longer backward calculation times would not meaningfully improve model performance.

Moisture sources above the PBL (41%) are not considered in this approach. This underestimate is inherent in the Lagrangian approach and therefore inevitable (e.g., Langhamer et al., 2018; Schuster et al., 2021; Sodemann & Zubler, 2009; Sodemann et al., 2008). How to deal with moisture uptake above the PBL is still controversial. There are studies which apply the same methodology and either consider moisture uptake in the free atmosphere as well (e.g., Baker et al., 2015; Fremme & Sodemann, 2019; Yao et al., 2020) or simply do not mention this issue when discussing the model performance (e.g., Bohlinger et al., 2017). Sub-grid scale processes, such as convection, are parameterized in the reanalysis model and might be one of the reasons for the non-physical moisture increase of trajectories above the scaled PBL. The PBL height might be underrepresented in numerical weather prediction models, especially over complex mountain terrains, where the vertical moisture flux deviates from observations (Weigel et al., 2007). This might explain the moisture increase within the free atmosphere. Sodemann and Zubler (2009) suggest a comparison of the moisture uptake patterns from inside the scaled PBL and the free troposphere. If the pattern shows similarities, the moisture origin from above the PBL can be seen as "unlikely to be fundamentally different from that of the accounted precipitation". However, clear evidence for their validation and a justification by those authors who not distinguish between moisture uptakes within the PBL and the free troposphere are missing.

5. Conclusions

Based on reanalysis data of the numerical weather prediction model ERA-Interim we applied a moisture source detection technique after Sodemann et al. (2008) to detect the moisture sources of the Crimean peninsula over the period from February 1979 to January 2017. The 15-days backward trajectories start at a regular grid (Figure 1) which covers the precipitable water of the Crimean peninsula. This approach assigns the moisture uptake to a particular region only if the specific humidity increases during a 6 h trajectory calculation time step within the scaled PBL height. On this setup the method identified the origin of 54% of the moisture which is responsible for precipitation on the Crimean peninsula, in the Lagrangian perspective. The applied moisture source identification technique considers for each identified moisture uptake along the trajectory the amount of pre-existing water and en-route precipitation. We conclude that contribution of moisture originating from the Atlantic Ocean is lower than previously thought (Vyed', 2000). There is an

interplay between the three major marine moisture sources, the Mediterranean Sea, Black Sea, and the Atlantic Ocean, which show comparable contributions to the Crimean precipitation (Figure 7). The following major marine moisture sources sorted by their contribution have been diagnosed:

1. The Mediterranean See contributes 15.3[13.9, 16.6]% of the total detectable moisture to the Crimean precipitation. On average, the air masses need 6 days to reach the target area. Actual travel times may vary from 1 to 9 days.
2. The Black Sea is the second-largest moisture source. It contributes 14.4[13.6, 15.2]% to the total detectable moisture. On average, the air masses need 2 days to reach the target area. The Black Sea has the smallest surface area of all main moisture sources but its location in the immediate vicinity provides for less en-route precipitation and the highest trajectory density.
3. The Atlantic Ocean contributes 13.9[12.7, 15.1]% of moisture. It is the most remote moisture source. En-route precipitation considerably reduces the contribution from this source. On average, the air parcels travel 10 days which is on the upper limit of the residence time of water within the atmosphere.

Taken together, the continental sources contribute 46.9[45.1, 48.6]% of the detectable moisture. More moisture originates from the European continent (32.0[30.4, 33.7]%) than from the southern continental moisture source (14.9[13.9, 15.8]%).

While the monthly precipitation amounts for the peninsula exhibit little seasonal fluctuations (Figure 1), seasonally dependent patterns are apparent in the sources of moisture (Figure 8). Winter months are characterized by enhanced moisture uptake from the Mediterranean Sea and Atlantic Ocean, where the core westerly storm track extends to 35°N and air on average, needs 1 day less to advect from the Atlantic Ocean. Due to the inhibited convectivity above land surfaces during cold months, continental moisture recycling reaches its seasonal minimum during winter (24.7[23.8, 25.7]%). The Mediterranean Sea and southern continental moisture sources are positively correlated with the monthly precipitation amounts. This highlights the role of the Mediterranean Sea as marine moisture source, and that of North-Africa being the favored storm track during moist winter months. Spring shows a transition pattern. Noticeable is the enhanced moisture uptake from the southern continental sources which is in accordance with the increased cyclonic density over the Anatolian Plateau during spring (Campins et al., 2011). Most of the moisture in summer originates from the European continent (54.6[52.3, 56.8]%) without showing any significant relation with the monthly precipitation amounts. This season is characterized by no predominant air advection. Autumn shows a large-scale flow pattern comparable to spring. However, higher sea surface and air temperatures at the Mediterranean and Black Seas during autumn obviously increase their contributions relative to spring. In particular, the dominant moisture contributors during spring are the Black Sea (20.4[18.7, 22.0]%), the Mediterranean Sea (17.8[15.3, 20.3]%) and continental moisture recycling (39.6[37.6, 41.6]%).

The moisture supply from the Mediterranean Sea and moisture uptake from AAA regions have a significant weak positive correlation to the monthly precipitation amounts, $R = 0.27$ and $R = 0.12$, respectively (Figure 9). The heaviest precipitation months, considering the 90% percentile, indicate the Mediterranean Sea as the major marine moisture contributor in these rare cases (20.6[15.5, 25.8]%). Contributions from the Black Sea, show an inverse relationship to the monthly precipitation amount ($R = -0.35$). Moisture originating from the Black Sea has a higher contribution during drier months.

In contrast to the reported long-term rising sea surface temperatures of the Mediterranean and Black Seas and the change of their net evaporation (e.g., Meredith et al., 2015; Pisano et al., 2020; Romanou et al., 2010; Skliris et al., 2018; Voskresenskaya & Vyshkvarkova, 2016), there is no evidence for a temporal trend in terms of the amounts or changing contributions from different moisture source regions between 1979 and 2017. Correlations between the Crimean monthly precipitation and the NAO index, and moisture sources (Mediterranean Sea, Black Sea, and southern continental moisture recycling) and the NAO index, exist only during winter. These findings are in agreement with stable water isotope results from the Crimean precipitation which indicate a significant negative correlation to the NAO index during winter (Dublyansky et al., 2018). In addition, there exists a significant positive correlation between the NAO index and the amount of moisture uptake from the Atlantic Ocean in spring ($R = 0.32$).

It can be concluded that moisture advected from the south and/or south-west results in very moist months at the Crimean peninsula. Future studies might focus on the occurrence of atmospheric rivers embedded in

the westerly storm track and their relation to both the overall precipitation characteristics and the extreme precipitation events.

Data Availability Statement

The ERA-Interim reanalysis data can be retrieved from the European Center for Medium-Range Weather Forecasts https://www.ecmwf.int/en/forecasts/datasets/reanalysis-datasets/era-interim. Data from the meteorological stations are available from NOAA https://www.ncdc.noaa.gov/cdo-web/datatools/findstation. We are happy to provide the monthly moisture sources of the Crimean peninsula obtained from the Lagrangian diagnostic (1979–2017) to interested researchers. The data is available via Zenodo: https://zenodo.org/deposit/4543535.

Acknowledgments
The authors gratefully acknowledge the support of Georg J. Mayr (Department of Atmospheric and Cryospheric Sciences, University of Innsbruck). Without the computational facilities provided by his working group, a study on this scale would never have been possible. The interdisciplinary collaborative work was motivated by Christoph Spötl (Institute of Geology, University of Innsbruck), whom the authors thank for this initiative and outstanding encouragement. We acknowledge support by the German Research Foundation (DFG) and the Open Access Publication Fund of Humboldt-Universität zu Berlin. Open access funding enabled and organized by Projekt DEAL.

References

Baker, A. J., Sodemann, H., Baldini, J. U. L., Breitenbach, S. F. M., Johnson, K. R., van Hunen, J., & Zhang, P. (2015). Seasonality of westerly moisture transport in the East Asian summer monsoon and its implications for interpreting precipitation $\delta^{18}O$. *Journal of Geophysical Research: Atmospheres*, *120*(12), 5850–5862. https://doi.org/10.1002/2014jd022919

Berrisford, P., Dee, D. P., Poli, P., Brugge, R., Fielding, M., Fuentes, M., & Simmons, A. (2011). *The ERA-interim archive version 2.0*. Shinfield Park: ECMWF Series: ERA Report.

Bohlinger, P., Sorteberg, A., & Sodemann, H. (2017). Synoptic conditions and moisture sources actuating extreme precipitation in Nepal. *Journal of Geophysical Research: Atmospheres*, *122*(23). https://doi.org/10.1002/2017jd027543

Buzzi, A., & Tibaldi, S. (1978). Cyclogenesis in the lee of the Alps: A case study. *Quarterly Journal of the Royal Meteorological Society*, *104*(440), 271–287. https://doi.org/10.1002/qj.49710444004

Campins, J., Genovés, A., Picornell, M. A., & Jansà, A. (2011). Climatology of Mediterranean cyclones using the ERA-40 dataset: Climatology of Mediterranean cyclones using the ERA-40. *International Journal of Climatology*, *31*(11), 1596–1614. https://doi.org/10.1002/joc.2183

Ciric, D., Nieto, R., Losada, L., Drumond, A., & Gimeno, L. (2018). The Mediterranean moisture contribution to climatological and extreme Monthly continental precipitation. *Water*, *10*(4), 519. https://doi.org/10.3390/w10040519

Dee, D. P., Uppala, S. M., Simmons, A. J., Berrisford, P., Poli, P., Kobayashi, S., et al. (2011). The ERA-interim reanalysis: Configuration and performance of the data assimilation system. *Quarterly Journal of the Royal Meteorological Society*, *137*(656), 553–597. https://doi.org/10.1002/qj.828

Dublyansky, Y. V., Klimchouk, A. B., Tokarev, S. V., Amelichev, G. N., Langhamer, L., & Spötl, C. (2018). Stable isotopic composition of atmospheric precipitation on the Crimean Peninsula and its controlling factors. *Journal of Hydrology*, *565*, 61–73.

Dzhamalov, R. G., Egorov, F. B., & Safronova, T. I. (2018). Groundwater resources and their role in water supply to Crimea. *Water Resources*, *45*(6), 839–845. https://doi.org/10.1134/s0097807818060052

Ergina, E. I., & Zhuk, V. O. (2019). Spatiotemporal variability of the climate and dangerous hydrometeorological phenomena on the Crimean Peninsula. *Russian Meteorology and Hydrology*, *44*(7), 494–500. https://doi.org/10.3103/s1068373919070082

Fremme, A., & Sodemann, H. (2019). The role of land and ocean evaporation on the variability of precipitation in the Yangtze River valley. *Hydrology and Earth System Sciences*, *23*(6), 2525–2540. https://doi.org/10.5194/hess-23-2525-2019

Gao, L., Bernhardt, M., & Schulz, K. (2012). Elevation correction of ERA-Interim temperature data in complex terrain. *Hydrology and Earth System Sciences*, *16*(12), 4661–4673. https://doi.org/10.5194/hess-16-4661-2012

Hurrell, J. W. (1995). Decadal trends in the North Atlantic oscillation: Regional temperatures and precipitation. *Science*, *269*(5224), 676–679. https://doi.org/10.1126/science.269.5224.676

Hurrell, J. W., Kushnir, Y., Ottersen, G., & Visbeck, M. (2003). An overview of the North Atlantic oscillation. *Geophysical Monograph-American Geophysical Union*, *134*, 1–36. https://doi.org/10.1029/134gm01

Kalnay, E. (2003). *Atmospheric modeling, data assimilation and predictability*. Cambridge University Press.

Kayukova, E. P., & Yurovsky, Y. G. (2017). Water resources of the Crimea. *Water Resources*, *44*(7), 886–891. https://doi.org/10.1134/s0097807817070053

Langhamer, L., Sauter, T., & Mayr, G. J. (2018). Lagrangian detection of moisture sources for the southern Patagonia Icefield (1979–2017). *Frontiers of Earth Science*, *6*, 219. https://doi.org/10.3389/feart.2018.00219

Logvinova, K. T., & Barabash, M. B. (1982). *Climate and hazardous hydrometeorological features of Crimea* (p. 317). Leningrad: Godrometeoizdat.

Meredith, E. P., Semenov, V. A., Maraun, D., Park, W., & Chernokulsky, A. (2015). Crucial role of Black Sea warming in amplifying the 2012 Krymsk precipitation extreme. *Nature Geoscience*, *8*(8), 615–619. https://doi.org/10.1038/ngeo2483

Owens, R., & Hewson, T. (2018). *ECMWF forecast user guide*. ECMWF. https://doi.org/10.21957/m1cs7h

Pachauri, R. K., Mayer, L., & on Climate Change, I. P. (2015). *Climate change 2014: Synthesis report*. Geneva: Intergovernmental Panel on Climate Change.

Pfahl, S., Madonna, E., Boettcher, M., Joos, H., & Wernli, H. (2014). Warm conveyor belts in the ERA-interim dataset (1979–2010). Part II: Moisture origin and relevance for precipitation. *Journal of Climate*, *27*(1), 27–40. https://doi.org/10.1175/jcli-d-13-00223.1

Pisano, A., Marullo, S., Artale, V., Falcini, F., Yang, C., Leonelli, F. E., & Buongiorno Nardelli, B. (2020). New evidence of Mediterranean climate change and variability from sea surface temperature observations. *Remote Sensing*, *12*(1), 132. https://doi.org/10.3390/rs12010132

Reynolds, R. W., Smith, T. M., Liu, C., Chelton, D. B., Casey, K. S., & Schlax, M. G. (2007). Daily high-resolution-blended analyses for sea surface temperature. *Journal of Climate*, *20*(22), 5473–5496. https://doi.org/10.1175/2007jcli1824.1

Romanou, A., Tselioudis, G., Zerefos, C. S., Clayson, C.-A., Curry, J. A., & Andersson, A. (2010). Evaporation-precipitation variability over the Mediterranean and the Black Seas from satellite and reanalysis estimates. *Journal of Climate*, *23*(19), 5268–5287. https://doi.org/10.1175/2010jcli3525.1

Schuster, L., Maussion, F., Langhamer, L., & Moseley, G. E. (2021). Lagrangian detection of precipitation moisture sources for an arid region in northeast Greenland: Relations to the North Atlantic oscillation, sea ice cover, and temporal trends from 1979 to 2017. *Weather and Climate Dynamics*, *2*(1), 1–17. https://doi.org/10.5194/wcd-2-1-2021

Shapiro, S. S., & Wilk, M. B. (1965). An analysis of variance test for normality (complete samples). *Biometrika*, *52*(3/4), 591–611. https://doi.org/10.2307/2333709

Skliris, N., Zika, J. D., Herold, L., Josey, S. A., & Marsh, R. (2018). Mediterranean Sea water budget long-term trend inferred from salinity observations. *Climate Dynamics*, *51*(7–8), 2857–2876. https://doi.org/10.1007/s00382-017-4053-7

Sodemann, H., Schwierz, C., & Wernli, H. (2008). Interannual variability of Greenland winter precipitation sources: Lagrangian moisture diagnostic and North Atlantic oscillation influence. *Journal of Geophysical Research*, *113*(D3). https://doi.org/10.1029/2007jd008503

Sodemann, H., & Zubler, E. (2009). Seasonal and inter-annual variability of the moisture sources for Alpine precipitation during 1995–2002. *International Journal of Climatology*, *30*(7), 947–961. https://doi.org/10.1002/joc.1932

Sprenger, M., & Wernli, H. (2015). The LAGRANTO Lagrangian analysis tool—version 2.0. *Geoscientific Model Development*, *8*(8), 2569–2586. https://doi.org/10.5194/gmd-8-2569-2015

Stohl, A., Haimberger, L., Scheele, M. P., & Wernli, H. (2001). An intercomparison of results from three trajectory models. *Meteorological Applications*, *8*(2), 127–135. https://doi.org/10.1017/s1350482701002018

Stohl, A., & James, P. (2004). A Lagrangian analysis of the atmospheric Branch of the global water cycle. Part I: Method description, validation, and demonstration for the August 2002 flooding in central Europe. *Journal of Hydrometeorology*, *5*(4), 656–678. https://doi.org/10.1175/1525-7541(2004)005<0656:alaota>2.0.co;2

Trigo, R. M., Osborn, T. J., & Corte-Real, J. M. (2002). The North Atlantic oscillation influence on Europe: Climate impacts and associated physical mechanisms. *Climate Research*, *20*(1), 9–17. https://doi.org/10.3354/cr020009

van der Ent, R. J., & Tuinenburg, O. A. (2017). The residence time of water in the atmosphere revisited. *Hydrology and Earth System Sciences*, *21*(2), 779–790. https://doi.org/10.5194/hess-21-779-2017

Vasilenko, V. A. (2017). Hydro-economic problems of Crimea and their solutions. *Regional Research of Russia*, *7*(1), 89–96. https://doi.org/10.1134/s2079970516040146

Vicente-Serrano, S. M., & López-Moreno, J. I. (2008). Nonstationary influence of the North Atlantic oscillation on European precipitation. *Journal of Geophysical Research*, *113*(D20). https://doi.org/10.1029/2008jd010382

Voskresenskaya, E., & Vyshkvarkova, E. (2016). Extreme precipitation over the Crimean Península. *Quaternary International*, *409*, 75–80. https://doi.org/10.1016/j.quaint.2015.09.097

Vyed', I. P. (1999). *Meso- and microclimatic variability of Crimea. Biologicheskoje i landshaftonje razonnbrazije Kryma: Problem i perspektivi*. Simferopol: Sonat.

Vyed', I. P. (2000). *Climatic atlas of Crimea. Supplement to "Questions of development of Crimea"* (p. 120). Simferopol: Tavrija-Plus.

Wanner, H., Brönnimann, S., Casty, C., Gyalistras, D., Luterbacher, J., Schmutz, C., & Xoplaki, E. (2001). North Atlantic oscillation-concepts and studies. *Surveys in Geophysics*, *22*(4), 321–381. https://doi.org/10.1023/a:1014217317898

Weigel, A. P., Chow, F. K., & Rotach, M. W. (2007). The effect of mountainous topography on moisture exchange between the "surface" and the free atmosphere. *Boundary-Layer Meteorology*, *125*(2), 227–244. https://doi.org/10.1007/s10546-006-9120-2

Wernli, B. H., & Davies, H. C. (1997). A Lagrangian-based analysis of extratropical cyclones. I: The method and some applications. *Quarterly Journal of the Royal Meteorological Society*, *123*(538), 467–489. https://doi.org/10.1002/qj.49712353811

Wilks, D. S. (2011). *Statistical methods in the atmospheric sciences* (Vol. 100). Academic press.

Winschall, A., Pfahl, S., Sodemann, H., & Wernli, H. (2014). Comparison of Eulerian and Lagrangian moisture source diagnostics—The flood event in eastern Europe in May 2010. *Atmospheric Chemistry and Physics*, *14*(13), 6605–6619. https://doi.org/10.5194/acp-14-6605-2014

Yao, S., Jiang, D., & Zhang, Z. (2020). Lagrangian simulations of moisture sources for Chinese Xinjiang precipitation during 1979–2018. *International Journal of Climatology*, *41*, E216–E232. https://doi.org/10.1002/joc.6679